A Case Study in the Molecular Interpretation of Optical Kerr Effect Spectra: Instantaneous-Normal-Mode Analysis of the OKE Spectrum of Liquid Benzene†

Seol Ryu and Richard M. Stratt*

Department of Chemistry, Brown University, Providence, Rhode Island 02912

Received: November 23, 2003; In Final Form: January 22, 2004

The ease with which optical Kerr effect (OKE) spectroscopy manages to sample dynamics in the far-infrared would seem to makes it a rather attractive way of doing intermolecular spectroscopy on liquids. However, molecular-level calculations of such spectra are still far less common than microscopically ill-defined phenomenological fits. As a result, there are comparatively few liquids whose OKE spectra have ever been interpreted in any genuinely molecular fashion. In this paper we explore the OKE spectrum of an experimentally well-studied liquid, liquid benzene, at a fully microscopic level by making use of molecular dynamics simulation and an instantaneous-normal-mode analysis. As has often been noted, the long-time tail of the OKE signal is quantitatively accounted for by rotational diffusion (albeit a collective diffusion). Moreover, consistent with the usual expectations, the interaction-induced portion of the remaining signal (which we show to arise almost entirely from center-of-mass translation in this example) appears only at low frequency. However, contrary to the common assumptions, rotational dynamics, often strongly coupled with translational dynamics, contributes over the entire spectral range. The unusual shape of the experimental benzene OKE spectra is shown to arise from the presence of an especially large ratio of rotational to translational bandwidths, an explanation that may account for the similar spectra seen with numerous other planar molecules. Having a molecular-level picture also allows us to point out that there is no need to invoke any kind of hypothetical benzene aggregates in order to explain benzene's OKE spectrum. Benzene and related aromatics are simple liquids whose dynamics, as well as structure, depend largely on repulsive forces and molecular shape.

I. Introduction

Optical Kerr effect (OKE) spectroscopy (a kind of Fourier transform Raman spectroscopy) has established itself as one of the primary experimental routes for probing the intermolecular vibrations of liquids.[1] Although this approach is certainly not unique in its ability to study the 0−300 cm^{-1} range characteristic of typical intermolecular dynamics in liquids,[2−7] it seems particularly well adapted to doing so, as evidenced by the hundreds of applications that have been reported in the literature over the past decade.[8] The question we should be periodically re-asking, however, is precisely what lessons about molecular dynamics are we learning from this spectroscopy that we really want to know.

Fundamentally, what OKE spectra measure are correlation functions involving the anisotropic dynamics of the liquid's collective polarizability tensor $\vec{\vec{\Pi}}$. In particular, the response function for this (third-order) Raman process can be written[9]

$$R^{(3)}(t) = -\beta \frac{d}{dt}\langle \Pi_{xz}(t)\Pi_{xz}(0)\rangle \tag{1.1}$$

with $\beta = (k_B T)^{-1}$. The focus on the anisotropy guarantees that a significant fraction of the dynamics reported in an OKE spectrum involves some sort of molecular reorientation.[10] Still, there is remarkably little genuinely microscopic understanding of precisely which molecular motions contribute to the response at a given frequency. It is this basic idea of ascertaining the *molecular mechanisms* that generate the OKE signal that we want to explore in this paper.

† Part of the special issue "Hans C. Andersen Festschrift".

Part of the difficulty lies with the collective polarizability itself, a quantity that stems from both individual isolated-molecule (MOL) polarizabilities and interaction-induced (I−I) corrections to those polarizabilities.[9,11−13]

$$\vec{\vec{\Pi}} = \vec{\vec{\Pi}}_{MOL} + \vec{\vec{\Pi}}_{I-I} \tag{1.2}$$

$$\vec{\vec{\Pi}}_{MOL} = \sum_{j=1}^{N} \vec{\vec{\alpha}}(j) \tag{1.3}$$

Here, $j = 1, ..., N$ labels the molecules and $\vec{\vec{\alpha}}(j)$ denotes what the polarizability of the jth molecule would be in the absence of intermolecular interactions.

For rigid molecules the *only* way that $\vec{\vec{\alpha}}$ tensors can evolve in time is via molecular reorientation; rotating the principal molecular axes rearranges the elements of the molecule's polarizability tensor. However, almost any single-molecule, or collective, motion involving almost any translational or rotational degrees of freedom will lead to some time evolution of the interaction-induced terms. So, as with any light-scattering experiment it can be difficult to assign specific molecular origins to any specific spectroscopic features.[11]

Of course molecular dynamics simulations have no problem in separating the molecular and interaction-induced portions of OKE spectra.[13−19] It is straightforward to distinguish pure molecular from the pure interaction-induced (and the cross contributions from both of those) just by substituting eq 1.2 in eq 1.1 and collecting the terms of each sort. Moreover, it is even possible, as Frenkel and McTague showed,[11] and subsequent authors have elaborated,[16,18,19] to use formal projection

10.1021/jp0375665 CCC: $27.50
Published on Web 03/19/2004

schemes to separate out the fraction of the I−I signal that tracks the dynamics of the molecular signal. However, this kind of decomposition does not tell us much about the molecular mechanisms that produce the signal. The distinction between "molecular" and "interaction-induced" is simply a statement about how electromagnetic radiation couples to our system, not about the underlying liquid dynamics. (We might also note that even performing this limited an analysis on experimental signals is not straightforward. Indeed, one of the points we will make in this paper is that the functional forms commonly used to fit these portions of an OKE spectrum may be neither numerically accurate nor physically justifiable.)

The approach we take in this paper to getting at underlying molecular mechanisms makes use of instantaneous-normal-mode (INM) analysis.[20,21] The central idea here, as it has been in applying INM formalism to solute relaxation processes,[22] is to use the instantaneous normal modes—the eigenvectors of the liquid's mass-weighted potential-energy second-derivative matrix, evaluated at each instantaneous liquid configuration—as a basis set for representing the relevant liquid dynamics. Within the short-time assumptions characteristic of INM theory, it is possible to show that the frequency-domain version of eq 1.1 is proportional to an *influence spectrum* for the liquid, the probability density of INM modes weighted (in our case) by the efficiency of each mode at changing the anisotropic part of the collective polarizability. But, because the resulting spectrum is constructed out of molecularly well-defined pieces, we know unambiguously how to project out the specific contributions of any given set of molecular motions that we think might be responsible for some piece of the signal.

This basic notion of analyzing light-scattering spectroscopies by INM methods has been advanced before, both for third-[15,23−27] and fifth-order[26−29] Raman spectra. Here, however, we extend the previous efforts, illustrating how molecular mechanisms can be determined at finer and finer levels of detail. To make this point we choose to focus on liquid benzene, a frequent target of OKE investigations and a liquid whose somewhat unusual spectrum has long been a subject of speculation.[3−6,30−38]

The first detailed reports of benzene's OKE spectrum (and its equivalent induced-phase-modulation and depolarized-stimulated-gain spectra) were those of Hattori et al.,[3] Friedman, Lee, and She,[30] and McMorrow and Lotshaw[31] in the early 1990s. McMorrow and Lotshaw, in particular, noted that this spectrum (and that of fellow aromatic species, pyridine) have somewhat odd, flattened shapes at frequencies around 15 cm^{-1}, falling off much more slowly to the low-frequency side than the spectra of liquids such as CS_2. In view of the possibility of specific π interactions of aromatic molecules, they speculated that this feature might be the result of dimer or other small-cluster vibrations. Indeed, molecular beam studies have pointed out that the Raman spectra of small benzene clusters have peaks in much the same low-frequency region,[39] lending plausibility to this explanation.

Similar kinds of flattened peaks and low-frequency structure began to be seen in OKE measurements of other aromatic liquids as well. Aniline,[40] benzonitrile,[32,40,41] and toluene[5,41] all seem to display analogous behaviors. There was, of course, the possibility that because these species were asymmetric tops, one was simply seeing the different rotational possibilities opened up by having distinct moments of inertia around the most spectroscopically active rotational axes—the same explanation that has been offered for the somewhat higher frequency differences seen in the spectra of benzene, chlorobenzene, bromobenzene, and iodobenzene[4,42] as well as for the low-frequency characteristics of other aromatic and nonaromatic ring compounds.[4,32,34] However, in 1997 Quitevis and co-workers[34] showed that the manifestly symmetric species hexafluorobenzene was quite similar to benzene in having an unusual low-frequency spectrum. These authors were, if anything, even more direct in attributing their findings to specific localized dimer motions.

From a liquid-theory perspective, much of this analysis seems rather few-body in character, as well as being tied inordinately closely to the specifics of the intermolecular pair attractions. Both of these aspects are somewhat disquieting. The equilibrium structure of simple liquids such as benzene is determined predominantly by cooperative packing, not by the particulars of the two-body attractive forces.[43,44] One would not even expect the relative orientations of neighboring molecules in a liquid to be the same as one sees in small clusters. There have, accordingly, been alternative explanations proffered that do have more of a many-body flavor. Both Bartolini et al.[42] and Ratajska-Gadomska[38] proposed that the low-frequency responses reflected collective, phonon-like, intermolecular vibrations. It has also been suggested that the peculiarities of the spectral shape arise from some kind of motional narrowing.[36,37] Here again, though, we can see the price paid for not having a definitive molecular picture of the spectroscopy. Phrases such as "motional narrowing" are valuable for well-defined degrees of freedom, carbonyl stretching vibrations or nuclear spins, for example, perturbed by their surroundings. But in the absence of some specific degree of freedom coupled to some physically identifiable bath, the concept is of only limited utility. In particular, if we are going to say that *intermolecular* motion is motionally narrowed, we need to be specific about just what plays the role of the surrounding coordinates.[45]

In the remainder of this paper we look in depth at the specific molecular motions responsible for the OKE spectrum of benzene. Section II presents our instantaneous-normal-mode representation of the spectrum and lays out how we can extract the contributions of specific molecular degrees of freedom. Section III describes our particular model for the liquid (our choice of intermolecular potential and our approach to calculating the collective polarizability) and goes over a few calculational details. We finally turn, in section IV to the results of our study. Section V provides a summary of our findings along with a number of concluding remarks.

II. INM Analysis of OKE Spectra

II.A. Basic INM Theory for Liquids of Nonlinear Molecules. Since most of the INM applications to date have been to either atomic liquids or to liquids composed of linear molecules, we start with a brief review of how INM theory can be formulated for more general molecular liquids.[46] If we take the molecules to be rigid with molecular weight M, the classical Hamiltonian of a neat molecular liquid can be always be expressed as

$$\mathbf{H} = \sum_{j=1}^{N}\left(\frac{1}{2}M\dot{\mathbf{r}}_j^{\,2} + \frac{1}{2}\sum_{\gamma=x,y,z} I_{j\gamma}\omega_{j\gamma}^{\,2}\right) + V(\mathbf{R}) \qquad (2.1)$$

where $\mathbf{r}_j$ is the center-of-mass of the jth molecule ($j = 1, ..., N$) and $\omega_{j\gamma}$ and $I_{j\gamma}$ are the angular velocity and the moment of inertia about the γth body-fixed axis of the jth molecule. The last term in the Hamiltonian, the potential energy V, depends in general on the complete set of $6N$ coordinates

$$\mathbf{R} = \{\mathbf{r}_1, \Omega_1, ..., \mathbf{r}_N, \Omega_N\} \qquad (2.2)$$

with $\Omega_j = \{\phi_j, \theta_j, \psi_j\}$ the Euler angles defining the jth molecule's orientation.

Given an instantaneous liquid configuration $\mathbf{R}_0$ for such a liquid, we construct the instantaneous normal modes (INMs) by first defining the $6N$-dimensional mass-weighted translational and rotational coordinates. At any time t, we write

$$\mathbf{Z}_t = \{z_{j\mu}(t); j = 1, ..., N; \mu = 1, ..., 6\} \tag{2.3}$$

$$z_{j\mu} = \begin{cases} \sqrt{M} r_{jx}, \sqrt{M} r_{jy}, \sqrt{M} r_{jz} & (\mu = 1, 2, 3) \\ \sqrt{I_x}\, \zeta_{jx}, \sqrt{I_y} \zeta_{jy}, \sqrt{I_z} \zeta_{jz} & (\mu = 4, 5, 6) \end{cases} \tag{2.4}$$

with μ labeling the internal coordinates of each molecule and the instantaneous-molecular-frame angles $\zeta_{j\gamma}$ ($\gamma = x, y, z$) derived from the instantaneous rotation matrices

$$\begin{pmatrix} \zeta_{jx} \\ \zeta_{jy} \\ \zeta_{jz} \end{pmatrix} = \begin{pmatrix} \sin\theta_j^0 \sin\psi_j^0 & \cos\psi_j^0 & 0 \\ \sin\theta_j^0 \cos\psi_j^0 & -\sin\psi_j^0 & 0 \\ \cos\theta_j^0 & 0 & 1 \end{pmatrix} \begin{pmatrix} \phi_j \\ \theta_j \\ \psi_j \end{pmatrix} \tag{2.5}$$

Here, $\Omega_j^0 = \{\phi_j^0, \theta_j^0, \psi_j^0\}$ are the Euler angles at instantaneous configuration $\mathbf{R}_0$.

We can then express the INM Hamiltonian simply by writing its value at time t as an expansion about the instantaneous ($t = 0$) behavior:

$$\mathbf{H}(\mathbf{Z}_t, \dot{\mathbf{Z}}_t) = \frac{1}{2}\dot{\mathbf{Z}}_t \cdot \dot{\mathbf{Z}}_t + V(\mathbf{R}_0) - \mathbf{F}(\mathbf{R}_0)\cdot(\mathbf{Z}_t - \mathbf{Z}_0) + \frac{1}{2}(\mathbf{Z}_t - \mathbf{Z}_0)\cdot\boldsymbol{D}(\mathbf{R}_0)\cdot(\mathbf{Z}_t - \mathbf{Z}_0) \tag{2.6}$$

with the $6N$-dimensional force vector $\mathbf{F}(\mathbf{R}_0)$ and the $6N \times 6N$ dynamical matrix $\boldsymbol{D}(\mathbf{R}_0)$ just the instantaneous (negative) gradient and instantaneous Hessian matrix of the potential with respect to the mass-weighted coordinates

$$F_{j\mu}(\mathbf{R}_0) = [\mathbf{F}(\mathbf{R}_0)]_{j\mu} = -(\nabla_{j\mu} V)_{\mathbf{R}_0} \tag{2.7}$$

$$D_{j\mu,k\nu}(\mathbf{R}_0) = [\boldsymbol{D}(\mathbf{R}_0)]_{j\mu,k\nu} = (\nabla_{j\mu}\nabla_{k\nu} V)_{\mathbf{R}_0} \tag{2.8}$$

$$\nabla_{j\mu} \equiv \frac{\partial}{\partial z_{j\mu}}$$

The INMs themselves now arise automatically just from diagonalizing the instantaneous dynamical matrix. If $\boldsymbol{U}(\mathbf{R}_0)$ is the $6N \times 6N$ orthogonal matrix that diagonalizes $\boldsymbol{D}(\mathbf{R}_0)$, then any displacement from the instantaneous liquid configuration, $\mathbf{Z}_t - \mathbf{Z}_0$, can be thought of as a superposition of contributions from instantaneous normal modes $q_\alpha(t)$, ($\alpha = 1, ..., 6N$)

$$q_\alpha(t; \mathbf{R}_0) = \sum_{j\mu} U_{\alpha,j\mu}(\mathbf{R}_0)[z_{j\mu}(t) - z_{j\mu}(0)] \tag{2.9}$$

Moreover, because each mode is associated with an eigenvalue

$$\omega_\alpha{}^2(\mathbf{R}_0) = \sum_{j\mu,k\nu} U_{\alpha,j\mu}(\mathbf{R}_0) D_{j\mu,k\nu}(\mathbf{R}_0) U^{\mathrm{tr}}_{k\nu,\alpha}(\mathbf{R}_0) \tag{2.10}$$

which tells us the mode's frequency ω_α, and an instantaneous force, which prescribes the initial stress acting on the mode

$$f_\alpha(\mathbf{R}_0) = \sum_{j\mu} U_{\alpha,j\mu}(\mathbf{R}_0) F_{j\mu}(\mathbf{R}_0) \tag{2.11}$$

we find that entire Hamiltonian, eq 2.6, can always be rewritten in INM form, as a sum over independent, shifted harmonic oscillators

$$\mathbf{H} = V(\mathbf{R}_0) + \sum_{\alpha=1}^{6N}\left(\frac{1}{2}\dot{q}_\alpha{}^2 + \frac{1}{2}\omega_\alpha{}^2 q_\alpha{}^2 - f_\alpha q_\alpha\right) \tag{2.12}$$

Even in advance of any detailed dynamical predictions, the structure of eq 2.12 is quite striking. Among other things it suggests that the distribution of mode frequencies (the liquid's *density of states*)

$$D(\omega) = \left\langle \frac{1}{6N}\sum_{\alpha=1}^{6N} \delta(\omega - \omega_\alpha) \right\rangle \tag{2.13}$$

(where the brackets indicate an equilibrium average over the exact Hamiltonian, eq 2.1) will give us a quantitative description of the natural range of time scales characterizing the liquid's motion.

II.B. INM Evaluation of OKE Spectra. The dynamics implied by the Hamiltonian eq 2.12 is, of course, easy to evaluate. In terms of the shifted modes

$$x_\alpha(t; \mathbf{R}_0) = q_\alpha(t; \mathbf{R}_0) - \frac{f_\alpha(\mathbf{R}_0)}{\omega_\alpha{}^2(\mathbf{R}_0)} \tag{2.14}$$

the Hamiltonian becomes

$$\mathbf{H} = V(\mathbf{R}_0) + \sum_{\alpha=1}^{6N}\left(\frac{1}{2}\dot{x}_\alpha{}^2 + \frac{1}{2}\omega_\alpha{}^2 x_\alpha{}^2 - \frac{f_\alpha{}^2}{2\omega_\alpha{}^2}\right) \tag{2.15}$$

meaning that each mode undergoes simple harmonic motion, although it does so with somewhat unusual, configuration-dependent, initial conditions

$$x_\alpha(t; \mathbf{R}_0) = x_\alpha(0)\cos\omega_\alpha t + \frac{v_\alpha(0)}{\omega_\alpha}\sin\omega_\alpha t \tag{2.16a}$$

$$v_\alpha(t; \mathbf{R}_0) = \dot{x}_\alpha(t; \mathbf{R}_0) = v_\alpha(0)\cos\omega_\alpha t - \omega_\alpha x_\alpha(0)\sin\omega_\alpha t \tag{2.16b}$$

$$x_\alpha(0) \equiv -\frac{f_\alpha}{\omega_\alpha{}^2}; \quad \mathrm{v}_\alpha(0) \equiv \dot{x}_\alpha(t = 0; \mathbf{R}_0) \tag{2.17}$$

To turn this information into a prediction for the OKE response function, eq 1.1, we simply need to express the time evolution of the many-body polarizability in terms of this INM basis.[15,23−27] For short enough times a linear approximation suffices[15,24]

$$\Pi_{xz}(t) - \Pi_{xz}(0) \approx \sum_\alpha \Pi_{xz,\alpha} q_\alpha(t) \tag{2.18}$$

$$\Pi_{xz,\alpha} \equiv \left(\frac{\partial \Pi_{xz}}{\partial q_\alpha}\right)_{\mathbf{R}_0} = \sum_{j\mu} U_{\alpha,j\mu}(\mathbf{R}_0)\left(\frac{\partial \Pi_{xz}}{\partial z_{j\mu}}\right)_{\mathbf{R}_0} \tag{2.19}$$

so by using eqs 2.14 and 2.16 and averaging over initial conditions, eq 2.17, we find that we can express the response in terms of an OKE *influence spectrum*, $\rho^{xzxz}(\omega)$, a density of states weighted by the ability of each mode to influence the liquid's many-body polarizability

$$\frac{\mathrm{d}}{\mathrm{d}t}\mathrm{R}^{(3)}(t) = \beta\langle\dot{\Pi}_{xz}(t)\dot{\Pi}_{xz}(0)\rangle = \int_0^\infty \mathrm{d}\omega\, \rho^{xzxz}(\omega)\cos\omega t \tag{2.20}$$

$$\rho^{xzxz}(\omega) = \langle \sum_{\alpha} (\Pi_{xz,\alpha})^2 \delta(\omega - \omega_\alpha) \rangle \tag{2.21}$$

In the frequency domain, this connection with the influence spectrum becomes even more direct. Equation 2.20 implies that the experimental frequency-domain spectrum

$$\mathrm{Im}[\mathrm{R}^{(3)}(\omega)] = \int_0^\infty \mathrm{d}t\, \mathrm{R}^{(3)}(t) \sin \omega t \tag{2.22}$$

is actually proportional to what we might call the "modified" influence spectrum $\rho^{xzxz}(\omega)/\omega$.

$$\mathrm{Im}[\mathrm{R}^{(3)}(\omega)] = \frac{\pi}{2} \frac{\rho^{xzxz}(\omega)}{\omega} \tag{2.23}$$

Equation 2.23 is, in fact, the basic starting point for our analysis.

II.C. INM Analysis of Molecular Mechanisms. What makes this framework potentially useful is not so much that it provides an explicit prediction for the OKE spectrum (although being able to predict time-dependent results solely in terms of purely time-independent quantities is somewhat gratifying) but that it allows us to make precise statements about the microscopic origins of the spectrum.[15] In particular, we can make a clear separation between contributions to the polarizability (the *coupling* to the radiation field) and contributions to the *dynamics* that makes that coupling evolve in time.

Analyzing the *coupling* is straightforward, in that we need to make only a limited use of the liquid modes. Suppose we envision that the many-body polarizability can be divided into two physically separate terms, A and B:

$$\Pi_{xz}(t) = \Pi_{xz}^{\mathrm{A}}(t) + \Pi_{xz}^{\mathrm{B}}(t) \tag{2.24}$$

We might, for example, want to study the division into molecular and interaction-induced contributions (eq 1.2), or the distinction between local contributions (say, those coming only from each molecule and its immediate first-shell neighbors) and nonlocal contributions (the remainder). Because any partition of this sort will automatically divide the mode derivatives, eq 2.19, into A and B terms

$$\Pi_{xz,\alpha} = \Pi_{xz,\alpha}^{\mathrm{A}} + \Pi_{xz,\alpha}^{\mathrm{B}} \tag{2.25}$$

$$\Pi_{xz,\alpha}^{\mathrm{A}} = \left(\frac{\partial \Pi_{xz}^{\mathrm{A}}}{\partial q_\alpha}\right)_{\mathbf{R}_0}, \quad \Pi_{xz,\alpha}^{\mathrm{B}} = \left(\frac{\partial \Pi_{xz}^{\mathrm{B}}}{\partial q_\alpha}\right)_{\mathbf{R}_0} \tag{2.26}$$

the influence spectrum, eq, 2.21, will also be partitioned into its physical components

$$\rho^{xzxz}(\omega) = \rho_{\mathrm{AA}}^{xzxz}(\omega) + \rho_{\mathrm{BB}}^{xzxz}(\omega) + \rho_{\mathrm{cross}}^{xzxz}(\omega) \tag{2.27}$$

$$\rho_{\mathrm{AA}}^{xzxz}(\omega) = \langle \sum_{\alpha} (\Pi_{xz,\alpha}^{\mathrm{A}})^2 \delta(\omega - \omega_\alpha) \rangle$$

$$\rho_{\mathrm{BB}}^{xzxz}(\omega) = \langle \sum_{\alpha} (\Pi_{xz,\alpha}^{\mathrm{B}})^2 \delta(\omega - \omega_\alpha) \rangle$$

$$\rho_{\mathrm{cross}}{}^{xzxz}(\omega) = 2 \langle \sum_{\alpha} (\Pi_{xz,\alpha}{}^{\mathrm{A}})(\Pi_{xz,\alpha}{}^{\mathrm{B}}) \delta(\omega - \omega_\alpha) \rangle \tag{2.28}$$

affording us both a frequency-resolved perspective on the relative importance of the A and B contributions to the coupling and (via the cross term) a measurement of the independence of the two components.

The *dynamical* analysis, by contrast, needs to take advantage of our detailed knowledge of the precise contributions of each degree of freedom to each mode. Suppose A is now some set of liquid degrees of freedom whose role we want to assess, and B is the set containing all of the remaining degrees of freedom; perhaps the molecular translations and rotations (respectively), or perhaps the local and nonlocal *motions*. The mode derivatives of the coupling, eq 2.19, can still be partitioned as in eqs 2.25, 2.27, and 2.28. Now, however, we want our derivatives to be *projected* derivatives appropriate to each set of molecular motions

$$\Pi_{xz,\alpha}^{\mathrm{A}} = \sum_{j\mu \in \mathrm{A}} U_{\alpha,j\mu}(\mathbf{R}_0) \left(\frac{\partial \Pi_{xz}}{\partial z_{j\mu}}\right)_{\mathbf{R}_0}$$

$$\Pi_{xz,\alpha}^{\mathrm{B}} = \sum_{j\mu \in \mathrm{B}} U_{\alpha,j\mu}(\mathbf{R}_0) \left(\frac{\partial \Pi_{xz}}{\partial z_{j\mu}}\right)_{\mathbf{R}_0} \tag{2.29}$$

so that the resulting influence spectra will report on the relative importance (and independence) of selected pieces of the liquid dynamics at each frequency.[15,22]

As we have noted elsewhere, this kind of analysis can be thought of formally as an application of the projection operators (matrices) $\boldsymbol{P}^{\mathrm{A}}$ and $\boldsymbol{P}^{\mathrm{B}}$:[47]

$$(\boldsymbol{P}^{\mathrm{A}})_{\alpha\beta} = \sum_{j\mu \in \mathrm{A}} U_{\alpha,j\mu}(\mathbf{R}_0) U_{j\mu,\beta}^{\mathrm{tr}}(\mathbf{R}_0)$$

$$(\boldsymbol{P}^{\mathrm{B}})_{\alpha\beta} = \sum_{j\mu \in \mathrm{B}} U_{\alpha,j\mu}(\mathbf{R}_0) U_{j\mu,\beta}^{\mathrm{tr}}(\mathbf{R}_0) \tag{2.30}$$

$$\boldsymbol{P}^{\mathrm{A}} + \boldsymbol{P}^{\mathrm{B}} = \boldsymbol{1}, \quad (\boldsymbol{P}^{\mathrm{A}})^2 = \boldsymbol{P}^{\mathrm{A}}, \quad (\boldsymbol{P}^{\mathrm{B}})^2 = \boldsymbol{P}^{\mathrm{B}}, \quad \boldsymbol{P}^{\mathrm{A}}\boldsymbol{P}^{\mathrm{B}} = \boldsymbol{0} \tag{2.31}$$

where $\boldsymbol{1}$ is the unit matrix and $\boldsymbol{0}$ is the zero matrix. That is, eq 2.29 could just as well have been written

$$\Pi_{xz,\alpha}^{\mathrm{A}} = \sum_{\beta} (\boldsymbol{P}^{\mathrm{A}})_{\alpha\beta} \Pi_{xz,\beta}$$

$$\Pi_{xz,\alpha}^{\mathrm{B}} = \sum_{\beta} (\boldsymbol{P}^{\mathrm{B}})_{\alpha\beta} \Pi_{xz,\beta} \tag{2.32}$$

Writing our formalism in these terms not only makes it easy to see why our dynamical decomposition of the influence spectrum is unique (and not just merely plausible), it lets us find the dynamical components of the total density of states, $D(\omega)$, eq 2.13

$$D_{\mathrm{A}}(\omega) = \left\langle \frac{1}{6N} \sum_{\alpha} (\boldsymbol{P}^{\mathrm{A}})_{\alpha\alpha} \delta(\omega - \omega_\alpha) \right\rangle$$

$$D_{\mathrm{B}}(\omega) = \left\langle \frac{1}{6N} \sum_{\alpha} (\boldsymbol{P}^{\mathrm{B}})_{\alpha\alpha} \delta(\omega - \omega_\alpha) \right\rangle$$

$$D(\omega) = D_{\mathrm{A}}(\omega) + D_{\mathrm{B}}(\omega) \tag{2.33}$$

The main reason we introduce the formal projections in this paper, though, is that they suggest a new, somewhat deeper, level of analysis. The projections in eq 2.29 (or equivalently, eq 2.32) ask which liquid degrees of freedom are directly responsible for making the polarizability evolve. But individual degrees of freedom in liquids rarely act in isolation; they are invariably part of a more collective motion involving other, perhaps less spectroscopically visible, coordinates. So what we

really want when we are trying to understand the molecular origins of a spectroscopic signal at a given frequency ω is detailed information on that whole frequency-ω collective motion, weighted by its spectroscopic visibility. In INM terms that means for each frequency ω_α we are want to know, for each mode α, which spectroscopically dark motions D are *dynamically correlated* with which spectroscopically bright motions B.

Accordingly, by analogy with the projection operators defined in eq 2.30, suppose we have partitioned the dark coordinates, D, into two subsets, say D_1 and D_2, and we want to know which subset is more important. For each spectroscopically bright coordinate $j\mu$ we can define the relative weights $w_{\alpha,j\mu}$

$$w^{D_1}_{\alpha,j\mu} = \frac{\sum_{k\nu\in D_1}^{(k\nu\neq j\mu)} U_{\alpha,k\nu}U^{tr}_{k\nu,\alpha}}{\sum_{k\nu\neq j\mu} U_{\alpha,k\nu}U^{tr}_{k\nu,\alpha}}$$

$$w^{D_2}_{\alpha,j\mu} = \frac{\sum_{k\nu\in D_2}^{(k\nu\neq j\mu)} U_{\alpha,k\nu}U^{tr}_{k\nu,\alpha}}{\sum_{k\nu\neq j\mu} U_{\alpha,k\nu}U^{tr}_{k\nu,\alpha}}$$

$$w^{D_1}_{\alpha,j\mu} + w^{D_2}_{\alpha,j\mu} = 1 \tag{2.34}$$

making the analogue of eq 2.29 the (doubly) projected derivatives

$$\Pi^{B/D_1}_{xz,\alpha} = \sum_{j\mu\in B} U_{\alpha,j\mu}(\mathbf{R}_0)w^{D_1}_{\alpha,j\mu}(\mathbf{R}_0)\left(\frac{\partial\Pi_{xz}}{\partial z_{j\mu}}\right)_{\mathbf{R}_0}$$

$$\Pi^{B/D_2}_{xz,\alpha} = \sum_{j\mu\in B} U_{\alpha,j\mu}(\mathbf{R}_0)w^{D_2}_{\alpha,j\mu}(\mathbf{R}_0)\left(\frac{\partial\Pi_{xz}}{\partial z_{j\mu}}\right)_{\mathbf{R}_0} \tag{2.35}$$

Hence, the complete partitioning would be

$$\Pi_{xz,\alpha} = \Pi^{B}_{xz,\alpha} + \Pi^{D}_{xz,\alpha}$$

$$\Pi^{B}_{xz,\alpha} = \Pi^{B/D_1}_{xz,\alpha} + \Pi^{B/D_2}_{xz,\alpha}$$

$$\Pi^{D}_{xz,\alpha} = \Pi^{D_1}_{xz,\alpha} + \Pi^{D_2}_{xz,\alpha} \tag{2.36}$$

where the dark degrees of freedom have been subdivided in the traditional (eq 2.29) fashion, but the bright degrees of freedom have been classified according to which background coordinates their dynamics couples to most strongly.

At this stage one should, in principle, construct all 10 diagonal and cross contributions to the influence spectrum, eq 2.21. However, once we have explored the difference between bright and dark components of the influence spectra (via eq 2.28 for example), we can probably limit our subsequent calculations to a physically sensible, albeit somewhat arbitrary, decomposition of the bright part alone

$$\rho^{xzxz}_{BB}(\omega) = \rho^{xzxz}_{B/D_1}(\omega) + \rho^{xzxz}_{B/D_2}(\omega) \tag{2.37}$$

$$\rho^{xzxz}_{B/D_1}(\omega) = \langle\sum_\alpha (c^{B/D_1}_{xz,\alpha})^2\delta(\omega-\omega_\alpha)\rangle$$

$$\rho^{xzxz}_{B/D_2}(\omega) = \langle\sum_\alpha (c^{B/D_2}_{xz,\alpha})^2\delta(\omega-\omega_\alpha)\rangle \tag{2.38}$$

$$(c^{B/D_1}_{xz,\alpha})^2 \equiv (\Pi^{B/D_1}_{xz,\alpha})^2 + (\Pi^{B/D_1}_{xz,\alpha})(\Pi^{B/D_2}_{xz,\alpha})$$

$$(c^{B/D_2}_{xz,\alpha})^2 \equiv (\Pi^{B/D_2}_{xz,\alpha})^2 + (\Pi^{B/D_1}_{xz,\alpha})(\Pi^{B/D_2}_{xz,\alpha}) \tag{2.39}$$

To summarize then, what we are now poised to understand are three basic kinds of contributions to the OKE spectrum: the different components of the coupling of the molecular motions to the observable, the different molecular motions directly affecting the observable, and the different, hidden, molecular motions correlated with spectroscopically visible dynamics. Perhaps not surprisingly, we will actually find it useful to consider a few selected combinations of these projections as well.

III. Our Model and Computational Approach

III.A. Many-Body Polarizability. We can formulate the collective (many-body) polarizability of our liquid at a number of different levels, incorporating, if we so desire, some of the recent progress made in describing the details of charge fluctuations in the immediate vicinity of each molecule.[16,48] However, for the purposes of this paper we choose to adopt the standard point-dipole/induced-point-dipole (DID) model for the collective polarizability tensor $\vec{\vec{\Pi}}$, which expresses the liquid's total polarizability as a sum over the liquid-phase polarizabilities of the individual molecules j, each computed within the DID approximation[11,13]

$$\vec{\vec{\Pi}} = \sum_{j=1}^{N}\vec{\vec{\pi}}(j)$$

$$\vec{\vec{\pi}}(j) = \vec{\vec{\alpha}}(j)\cdot(\vec{\vec{1}} + \sum_{\substack{k=1\\k\neq j}}^{N}\vec{\vec{T}}_{jk}\cdot\vec{\vec{\pi}}(k)) \tag{3.1}$$

Here, $\vec{\vec{1}}$ is the unit tensor, $\vec{\vec{T}}_{jk}$ is the dipole-dipole tensor between molecules j and k

$$\vec{\vec{T}}_{jk} = [(3\hat{r}\,\hat{r} - \vec{\vec{1}})/r^3]_{\mathbf{r}=\mathbf{r}_{jk}} \tag{3.2}$$

and $\vec{\vec{\alpha}}(j)$, the isolated-molecule polarizability tensor for each molecule

$$\vec{\vec{\alpha}}(j) = \left(\alpha - \frac{\gamma}{3}\right)\vec{\vec{1}} + \gamma\,\hat{\Omega}_j\,\hat{\Omega}_j \tag{3.3}$$

is defined by its isotropic (α) and anisotropic (γ) parts and by the unit vector $\hat{\Omega}$ prescribing the principal symmetry axis of the molecule. For benzene we take the principal axis to be the 6-fold axis and assume $\alpha = 10.20$ Å^3 and $\gamma = -4.67$ Å^3.[49] To place these results in perspective we found it to be useful to repeat the calculations for liquid CS_2. When we did so we took the bonding axis to be the principal axis and assumed $\alpha = 8.95$ Å^3 and $\gamma = 10.05$ Å^3.[13,50]

In practice we evaluated the collective polarizability tensor by solving eq 3.1 iteratively (with the requirement that every element of each molecule's $\vec{\vec{\pi}}(j)$ be converged to within 0.001 Å^3). We also found it to be illuminating to compare the full

TABLE 1: Benzene Geometry and Pair Potential[a]

parameter	C−C	H−H	C−H	C	H
bond length (Å)	1.393	1.027			
pair potential parameters					
A (kJ Å^{-6} mol^{-1})	2439.8	136.4	576.9		
B (kJ mol^{-1})	369743	11971	66530		
C (Å^{-1})	3.60	3.74	3.67		
q (au)				−0.153	0.153

[a] Parameters for the Williams potential, eq 3.5 (ref 51). Benzene molecules are assumed to be perfectly hexagonal.

interaction-induced part computed in this fashion (eqs 1.2 and 1.3) with the first-order predictions

$$\vec{\pi}(j)^{(\text{1st order I−I})} = \vec{\alpha}(j)\cdot\sum_{\substack{k=1\\k\neq j}}^{N}\vec{\vec{T}}_{jk}\cdot\vec{\alpha}(k) \qquad (3.4)$$

As we shall show, the interaction-induced component of $\vec{\vec{\Pi}}$ for benzene is predicted quantitatively by this first-order formula. Liquid CS_2, by contrast, is not described nearly as well at this level of theory.[9,13,17] All of the calculations reported in this paper use the full interaction-induced polarizability, unless otherwise specified.

III.B. Intermolecular Potentials. Liquid benzene has been simulated with a variety of intermolecular potentials. Here again, though, we opt for a conventional choice, the frequently studied Williams potential,[51] a rigid model with a site located at each of the 12 atoms and an interaction between each site a on a molecule j and each site b on molecule k taken to be of the exp-6-plus-Coulomb form as a function of the site−site distance $r_{ja,kb} = |\mathbf{r}_{ja} - \mathbf{r}_{kb}|$

$$u_{ab}(r_{ja,kb}) = \left[B_{ab}\, e^{-C_{ab}r} - \frac{A_{ab}}{r^6} + \frac{q_a q_b}{r}\right]_{r=r_{ja,kb}} \qquad (3.5)$$

The molecular geometry, site charges q_a, and potential parameters A_{ab}, B_{ab} and C_{ab}, are given in Table 1.

Although the Williams model does not predict the correct T-shaped minimum-energy structure of the benzene dimer,[52] it has been shown to lead to liquid structures in good agreement with both neutron and X-ray diffraction.[53] Moreover, it also seems to do reasonably well when used to evaluate dielectric properties.[54] We should note, however, that there have been other 12-site rigid models with comparable behavior.[55−57] To help quantify the differences expected from the various potentials, we ran a series of molecular dynamics simulations to compare the predictions for several liquid correlation functions, as well as for the various diffusion constants. Table 2, in particular, shows the translational diffusion constant D, and the rotational diffusion constants about the 6-fold axis ($D_{||}$) and the 2-fold axes ($D_{\perp}$) taken from experimental measurements[58−65] and computed for four of the more common potentials.

With the exception of the results for rotation about the 6-fold axis ("spinning"), a process completely invisible to OKE spectroscopy, these numbers suggest that the Williams potential is a bit stiffer than the other potentials and, perhaps, somewhat stiffer than the real liquid. Both for rotation about the 2-fold axis ("tumbling") and for center-of-mass translation we find the Williams diffusion constants to be at the low end of the list. Admittedly, these kinds of zero-frequency observations need not have any direct bearing on the finite-frequency OKE studies, but angular velocity autocorrelation functions for the spinning motion (not shown) reveal that the Williams potential also exhibits the strongest backscattering.[66] The presumption is that these kinds of minor quantitative variations in interaction strength should have little effect on the molecular mechanisms used to generate the OKE spectrum, but it should not be too surprising when we find our predicted spectrum encompasses a somewhat larger range of frequencies than does the real experiment.

TABLE 2: Diffusion Constants for Liquid Benzene at 1 atm and 300 K: Experimental and Simulated Values[a]

diffusion constant	exptl[b]	Williams[c]	Califano[c]	Linse[c]	Jorgensen[c]
D (10^{-9} m^2 s^{-1})	2.28	1.15	1.66	2.55	1.45
$D_{\perp}$ (10^{10} s^{-1})	∼9	7.9	9.1	13.5	11.3
$D_{||}$ (10^{10} s^{-1})	∼20	27.3	33.3	27.5	22.6

[a] Values for center-of-mass diffusion (D), rotational diffusion about any 2-fold axis ($D_{\perp}$), and rotational diffusion about the 6-fold axis ($D_{||}$). The simulation results shown here were calculated by integrating the translational and rotational velocity autocorrelation functions; calculations for D based on mean-square displacements (not shown) gave values within 5% of the ones reported here. [b] Experimental results derived from NMR T_1 times and Raman line widths. D taken from refs 58 and 59; $D_{\perp}$ and $D_{||}$ values are an average over the results from refs 60−65. [c] Simulation results for the benzene potentials shown. The Williams potential is described in the text (ref 51), the Califano potential is of precisely the same form but with modified parameters (ref 55), the Linse potential is the sum of r^{-1}, r^{-4}, r^{-6}, r^{-9}, and r^{-12} terms (ref 56), and the Jorgensen potential is of the Lennard-Jones-plus-Coulomb form (ref 57).

Our comparison calculations on liquid CS_2 used the rigid-molecule, Lennard-Jones three-site potential of ref 67.

III.C. Molecular Dynamics and INM Details. Microcanonical molecular dynamics simulations of liquid benzene under ambient conditions (density 0.874 g/cm^3, temperature 300 K) were carried out with the MOLDY program, which uses a quaternion representation of the Euler angles and propagates the dynamics via a modified Beeman predictor−corrector algorithm.[68] Except where otherwise stated, the simulations employed $N = 108$ molecules, were carried out with Ewald summation evaluation of the electrostatic part of the intermolecular forces, and made use of periodic boundary conditions with a (half-simulation-cell) cutoff distance of 12.53 Å used for the polarizability tensors and all the nonelectrostatic interactions.[69] All of the calculations were performed with a time step of 5 fs.

After equilibrating the liquid, the OKE response functions were averaged over 4.7×10^5 choices for initial liquid configurations (separated from one another by 10 time steps). When we needed to obtain converged results for the long-time behavior, we used trajectories lasting 600 ps. Our INM calculations were averaged over 1.2×10^5 liquid configurations, also separated by intervals of 10 time steps.

As one of our first checks, we noted that the center-of-mass radial distribution functions resulting from these calculations were identical with those reported previously for the Williams potential.[53] The first peak appears at 5.5 Å, the first minimum at 7.7 Å, and the first shell (defined by integrating up to this minimum) contains an average of 12.6 neighboring molecules. We also noted that the 6-fold axes of these neighboring molecules were at an average angle of roughly 45° to one another. Indeed, as has long been appreciated, all of these near-neighbor statistics are quite consistent with what one would expect from a simple liquid whose structure was dominated by packing considerations.[43,44] There are certainly no obvious signs of any kind of dimer formation driven by intermolecular attraction, at least not within this model.

As a further check on the simulation quality, we also ran some simulations with $N = 256$ benzene molecules. The OKE

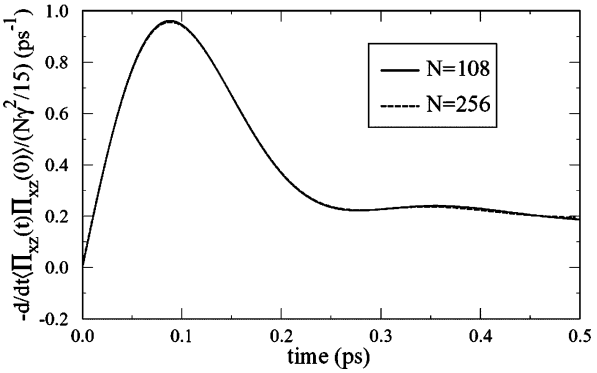

Figure 1. Simulated optical Kerr effect (OKE) response function for liquid benzene. The two curves, barely distinguishable on this scale, are the results of molecular dynamics simulations with $N = 108$ and 256 benzene molecules.

response functions computed with the larger sample turned out to be barely distinguishable from those of the smaller sample, Figure 1, in keeping with our observation that the OKE spectrum of benzene provides a rather localized perspective on benzene's dynamics.

Our comparison CS_2 simulations were carried out at a density of 1.26 g/cm^3 and a temperature of 300 K using $N = 256$ molecules and a time step of 1 fs, also with the MOLDY program.[68] Here we employed a 200 ps trajectory following equilibration and our INM results were averaged over 2×10^4 liquid configurations separated by 10 time-step intervals.

IV. Results

IV.A. Molecular Dynamics and the Overall Behavior. We begin our analysis by examining the outcome of a direct molecular dynamics simulation of eq 1.1, the OKE response function, plotted as the solid curves in Figure 2. The signal clearly has its largest contribution in the first few hundred femtoseconds, and indeed, this regime is where all the information about intermolecular vibrations resides. However, the lower panel in the figure reveals that there is also a lengthy, nearly single-exponential, decay that dominates the response once we get beyond a few picoseconds.

Given the time scale and given that OKE spectra look specifically at a liquid's anisotropy, it is natural to attribute this asymptotic decay to rotational diffusion.[1,8] In fact, one can be reasonably explicit about this expectation: Because (as has long been appreciated)[12,13] the interaction-induced polarizability dephases fairly quickly, the only long-time dynamics we should be able to see is that of the molecular part of the polarizability, eq 1.3. But if we substitute eqs 1.3 and 3.3 into eq 1.1 we find that the resulting response function reflects only the time-evolving directions of the molecular symmetry axes $\hat{\Omega}_j$

$$R^{(3)}(t) \sim -\beta\gamma^2 \frac{d}{dt}\langle \sum_{j,k} \Omega_j^x(0)\Omega_j^z(0)\Omega_k^x(t)\Omega_k^z(t)\rangle$$

and does so in much the same way as the liquid's P_2 (second-order-Legendre-polynomial) collective rotational correlation function

$$C_2(t) = \frac{1}{N}\langle \sum_{j,k=1}^{N} P_2[\hat{\Omega}_j(0)\cdot\hat{\Omega}_k(t)]\rangle \propto e^{-t/\tau_2} \qquad (4.1)$$

at least at long times. It is possible to show that, asymptotically[70]

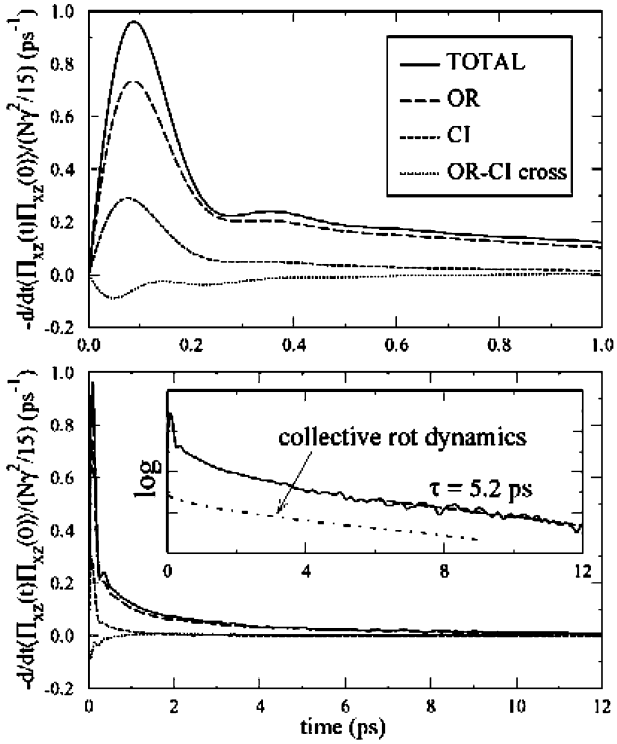

Figure 2. Molecular-dynamics-based partitioning of liquid benzene's OKE response function. The top and bottom panels show, on two rather different time scales, the total simulated response (TOTAL), its "orientational" component OR (the fraction of the total that is either single-molecule reorientation or dynamically correlated with that reorientation), its "collision-induced" component CI (the fraction of the interaction-induced response dynamically orthogonal to single-molecule reorientation), and its OR−CI cross correlation. The inset in the bottom panel shows the same total response given in the lower part of the panel, but on a logarithmic scale, emphasizing the linear behavior with slope $(5.2 \text{ ps})^{-1}$. As one can see from the inset, the collective rotational dynamics of the benzene molecules, eq 4.1, has precisely the same long-time behavior as the total response.

$$R^{(3)}(t) \rightarrow -N\frac{\beta\gamma^2}{15}\frac{d}{dt}C_2(t) \qquad (4.2)$$

which means that if C_2 has a single-exponential decay, both functions must have precisely the *same* single-exponential decay. Consistent with these expectations, the inset in Figure 2 shows that our collective rotational correlation function does have exactly the same single-exponential decay as our OKE response function and has exactly the same slope, $(\tau_2)^{-1} = (5.2 \text{ ps})^{-1}$.

Interestingly, the approach to this asymptotic behavior is well fit by adding a second exponential (not shown) whose time constant matches that of the noncollective (self) rotational correlation function, $(\tau_2^{\text{self}})^{-1} = (3.3 \text{ ps})^{-1}$.

$$C_2^{\text{self}}(t) = \frac{1}{N}\langle \sum_{j=1}^{N} P_2[\hat{\Omega}_j(0)\cdot\hat{\Omega}_j(t)]\rangle \propto e^{-t/\tau_2^{\text{self}}} \qquad (4.3)$$

We should point out that both of these rotational correlation times are noticeably longer than the experimental times, $\tau_2 = 2.84$ ps and $\tau_2^{\text{self}} = 2.71$ ps, that have been reported in the literature.[36] Still, these kinds of differences are not all that unexpected given the proclivity of the Williams potential to produce relatively small diffusion constants.[71]

Besides allowing us to separate out the purely diffusive components of the OKE signal, the other kind of information one can glean from a straightforward molecular dynamics

simulation is the precise distinction between signal coming from the molecular and the interaction-induced parts of the polarizability, eq 1.2. In fact, as Frenkel and McTague pointed out,[11] one can get a somewhat more sophisticated perspective on this information. Kiyohara et al. noted, for example, that by introducing dynamics into the original Frenkel−McTague scheme it was possible to compute the components of the molecular and interaction-induced pieces that remain independent of one another as time evolves.[18]

If we define the "dynamical overlap"

$$f(t) = \frac{\mathrm{Tr}[\vec{\vec{\Pi}}^{(2)}_{\mathrm{I-I}}(t)\cdot\vec{\vec{\Pi}}^{(2)}_{\mathrm{MOL}}(t)]}{\mathrm{Tr}[\vec{\vec{\Pi}}^{(2)}_{\mathrm{MOL}}(t)\cdot\vec{\vec{\Pi}}^{(2)}_{\mathrm{MOL}}(t)]} \tag{4.4}$$

where by the superscript (2) we mean the $L = 2$ spherical-tensor component for each tensor

$$\vec{\vec{\mathrm{F}}}^{(2)} = \vec{\vec{\mathrm{F}}} - \frac{1}{3}\mathrm{Tr}(\vec{\vec{\mathrm{F}}})\ \vec{\vec{1}} \tag{4.5}$$

then we can repartition the many-body polarizability into an "orientational" part (OR) composed of the molecular piece plus whatever elements of the interaction-induced piece there are that track the single-molecule rotational dynamics and a "collision-induced" part (CI) comprised of whatever elements of the interaction-induced piece there are that do *not* follow the purely molecular piece:

$$\begin{aligned}\vec{\vec{\Pi}}(t) &= \vec{\vec{\Pi}}_{\mathrm{OR}}(t) + \vec{\vec{\Pi}}_{\mathrm{CI}}(t)\\ \vec{\vec{\Pi}}_{\mathrm{OR}}(t) &= [1 + f(t)]\vec{\vec{\Pi}}_{\mathrm{MOL}}(t)\\ \vec{\vec{\Pi}}_{\mathrm{CI}}(t) &= \vec{\vec{\Pi}}_{\mathrm{I-I}}(t) - f(t)\vec{\vec{\Pi}}_{\mathrm{MOL}}(\mathrm{t})\end{aligned} \tag{4.6}$$

The reader can easily verify that this division is simply a reallocation of the two pieces in eq 1.2 but one that guarantees that the resulting terms are dynamically orthogonal to one another for all time

$$\mathrm{Tr}[\vec{\vec{\Pi}}^{(2)}_{\mathrm{CI}}(t)\cdot\vec{\vec{\Pi}}^{(2)}_{\mathrm{OR}}(t)] = 0$$

The results of this partitioning the OKE response in this fashion are also shown in Figure 2.

From these curves one can immediately see the roots of much of what is known about OKE spectroscopy. OKE responses are clearly largely orientational in character. The (manifestly nonorientational) collision-induced contribution are never more than a third of the response, and even that much lasts less than half a picosecond. Moreover, in accord with our earlier remarks, we see that once one gets beyond a picosecond (bottom panel) there is no discernible collision-induced response remaining in the signal.

IV.B. Global Instantaneous-Normal-Mode Analysis and the Nondiffusive Dynamics. Were we to stop at this point, we would know how to extract the diffusive dynamics from the OKE spectrum, but little more. To begin to examine the specific kinds of dynamics we are seeing on shorter time scales, we introduce the INM spectra of liquid benzene, Figure 3, which make an interesting comparison with the equivalent spectra of liquid carbon disulfide, Figure 4. Consider first the projections of the respective densities of states, eq 2.33.

Both C_6H_6 and CS_2 evidently have a natural frequency range for intermolecular motion of about 200 cm^{-1}, with center-of-mass translation concentrated in the first half of that range. What is different about the two liquids is the rotational dynamics.

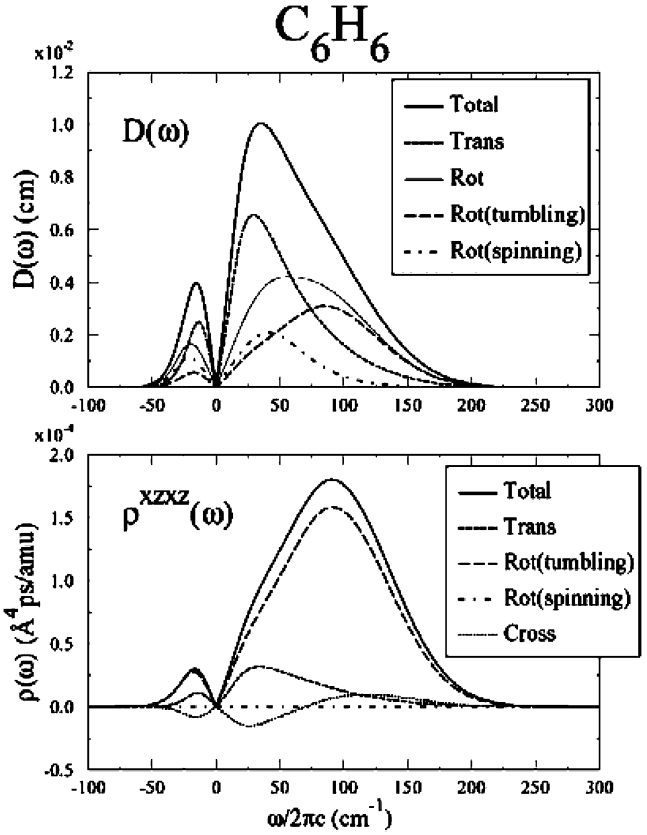

Figure 3. Instantaneous-normal-mode spectra for liquid benzene. We plot both the total density of states $D(\omega)$ and the total OKE influence spectrum $\rho^{xzxz}(\omega)$, along with their respective components arising from molecular translation (Trans) and rotation (Rot). The latter are further subdivided into contributions from reorientation about the 2-fold axes (tumbling) and about the 6-fold axis (spinning). Also shown for the influence spectrum are the translation−rotation cross components (Cross). Imaginary-mode contributions are displayed on the negative frequency axis, and the influence spectra are divided by the total number of modes so as to foster comparisons with the Figure 4.

Whereas the rotation of CS_2 largely overlaps its translation, only the spinning motion of benzene about its 6-fold axis has the same frequency range as its translation. The tumbling rotation about benzene's 2-fold axes seem to peak some 50 cm^{-1} higher.

The origin of these findings is actually almost entirely simple kinematics. The molecular weights of C_6H_6 (78 amu) and CS_2 (76 amu) are almost the same, giving the two liquids the same translational time scales. Similarly, the moment of inertia of CS_2 is quite close to that for the spinning motion of C_6H_6, but it is nearly twice that of benzene's tumbling motion. Much as had been seen in the INM densities of states of CH_3CN and liquid CO_2,[72] the details of the attractive intermolecular forces apparently play a remarkably small role in establishing the time scales of liquid motion.

Of course, the density of states tells us only these time scales. To make the connection with OKE spectroscopy we need to look at the bottom panels in these figures, the projected influence spectra, eqs 2.27−2.29. Here we find mostly what we learned from the molecular dynamics: the reorientational motions, whatever their frequencies, make the largest contributions to the OKE response.[15] Note, by the way, that the spinning motion is actually irrelevant to the OKE spectrum. Because it does not change the polarizability, it ends up being invisible in the influence spectrum.[37]

To begin to look more deeply into the actual molecular mechanisms behind the OKE signal suppose we reexamine these

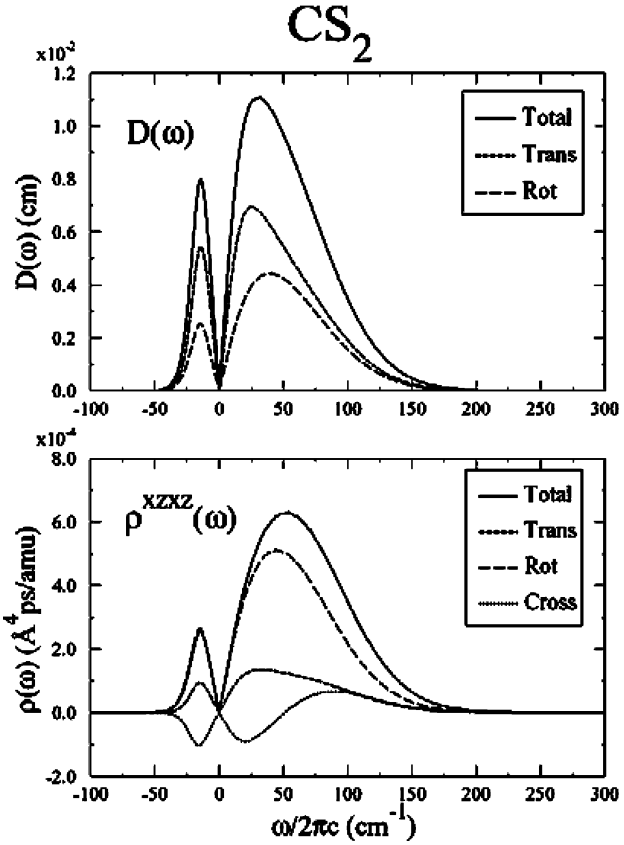

Figure 4. Instantaneous-normal-mode spectra for liquid carbon disulfide. Aside from the fact that all rotational motions are necessarily equivalent for a linear molecule, the curves shown here are the precise equivalent of those plotted in Figure 3. As with Figure 3, the influence spectrum is shown divided by the number of modes.

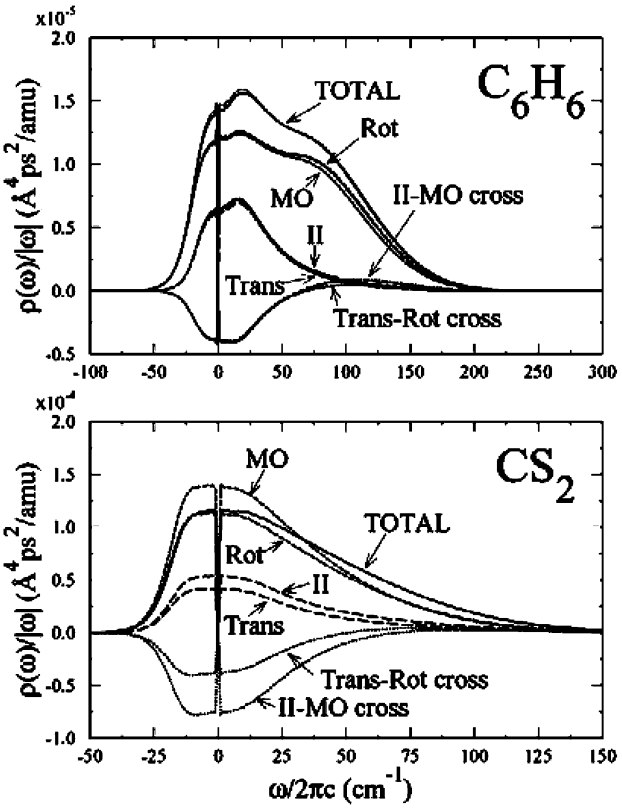

Figure 5. Modified OKE influence spectra for liquid benzene and liquid carbon disulfide, $\rho^{xzxz}(\omega)/\omega$, (which INM theory predicts ought to be proportional to the nondiffusive part of the frequency-domain OKE spectrum). Note the different frequency scales for the two liquids. For each spectrum, we show the contributions from molecular (MO) and interaction-induced (II) polarizability and we plot the results of projecting out the translational (Trans) and reorientational (Rot) liquid dynamics. The top panel also shows, as thin lines barely visible on this scale, the equivalent spectrum and spectral components for benzene when we include only the first-order dipole−induced-dipole contributions to the coupling. As is the case for all of the remaining figures, the imaginary-mode contributions (displayed on the negative frequency axis) merge continuously into the remainder of the plot.

influence spectra, but in the guise of the modified influence spectra that eq 2.23 tells should predict the (nondiffusive part of) the frequency-domain experimental spectra, Figure 5. The extra emphasis on low-frequency behavior created by dividing by ω seems to make it appear that translational dynamics has become more important. However, we also see that the translation−rotation cross term has been similarly magnified, and that these two terms substantially cancel one another, so rotation remains the major story. What is interesting, though, is the sudden appearance of a number of significant differences between benzene and carbon disulfide.

The biggest quantitative difference is the almost 2-fold diminishment in spectral range of carbon disulfide compared to that of benzene; the fact that CS_2 does not have the high-frequency librational dynamics of C_6H_6 has now become quite visible. But beyond that, we see that benzene is much closer to a simple, textbook example of an OKE spectrum than is carbon disulfide. Benzene's interaction-induced component apparently evolves in time almost entirely because of center-of-mass translation, and its molecular component follows virtually perfectly the liquid reorientational dynamics. Partly because CS_2 has significant high-order dipole−induced-dipole contributions to its polarizability, the dynamics driving the various pieces of the OKE response do not separate as cleanly.[9,13,17] Figure 5 shows that benzene, by contrast, is well described by a simple first-order DID treatment of the interaction-induced polarizability, eq 3.4.

There is another difference worth noting: the shape of the low-frequency response, the defining feature of benzene's unusual OKE spectrum. The predicted OKE spectrum of benzene displays a distinct peak and a shoulder, whereas CS_2's spectrum is smooth and featureless. Where does the benzene structure come from? A glance at the underlying dynamics makes it clear that whatever their detailed origin, these features are intimately connected with the level of separation between rotational and translational motion. Rotation and translation in CS_2 occur over the same frequency range, leading to a rather bland spectrum.[17,25] In benzene the high-frequency shoulder occurs just when the translational motion has died out, leaving us with a spectral shape that precisely mirrors the shape of the rotational (tumbling) contribution. At the 20 cm^{-1} or so where the low-frequency peak, appears in benzene, one does find both translational and rotational contributions, but intriguingly, both the rotational and translational components in the benzene case seem to have peaks of their own. One obviously needs to pursue this feature a little further.

IV.C. Local INM Analysis. The next question to ask, perhaps, is just how local a perspective do OKE spectra have? If we define the first shell around a benzene molecule as we did in section III, then it is possible to subdivide the many-body polarizability into the portions coming from the immediate neighborhood of each molecule (the molecule itself and its 12−13 first-shell neighbors) and the remainder. Applying eqs 2.24−2.28 with this division produces the top panel of Figure 6.

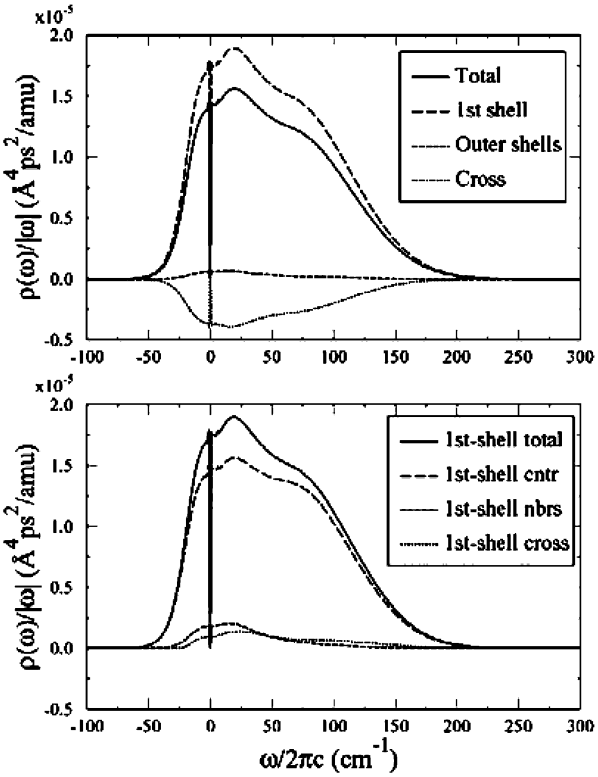

Figure 6. *First-shell contributions* to the modified OKE influence spectrum for liquid benzene. The top panel shows the outcome of assuming that only the first-shell neighbors of a molecule contribute to its interaction-induced polarizability (1st shell), of assuming that only the non-first-shell molecules contribute (Outer shells), and of the cross contributions (Cross). The bottom panel takes the first-shell curve (1st-shell total) and projects out the dynamical components arising from motion of the central molecule (1st-shell cntr) and the neighbors of the central molecule (1st-shell nbrs), as well as from the cross contribution between these two.

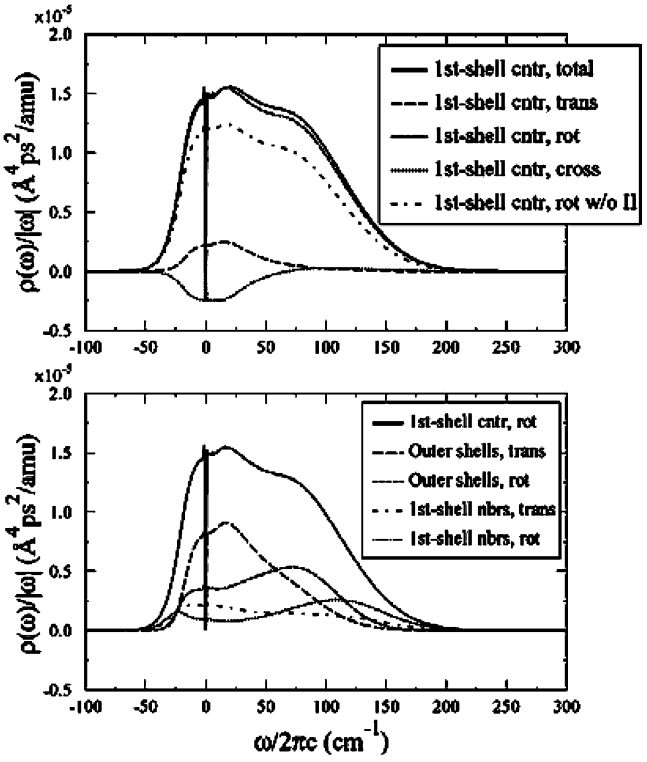

Figure 7. *First-shell-polarizability/central-molecule-dynamics contributions* to the modified OKE influence spectrum for liquid benzene. The figure starts with the spectrum one would get by neglecting the contributions of outer shells to the polarizability and of all but the central molecule to the dynamics (the 1st-shell cntr curve from Figure 7). The top panel then projects out the dynamical components arising from reorientational (rot) and center-of-mass translational (trans) motion of the central molecule, as well as presenting the cross contribution. The panel also shows how the rotational curve would appear if we completely ignored all of the interaction-induced contributions (rot w/o II). The bottom panel takes the center-molecule-rotation curve from the top panel (including the I−I contribution) and examines the dynamics of the *other* molecules participating in each contributing mode. In particular, the curve is partitioned into components according to whether it is the neighboring molecules within the first shell (1st-shell nbrs) or the molecules outside the first shell (Outer shells) that are moving and whether those molecules are translating (trans) or reorienting (rot).

Judging from the figure, it is clear that, at least in a qualitative sense, a first-shell picture captures the entire response. There is essentially no direct contribution from the outer shells; there is a modest negative first-shell/outer-shells cross term that acts to attenuate the signal a bit, but it hardly seems to affect its shape. So what of the dynamics within these cluster-like segments? Assuming that each "cluster" is independent could obviously lead to overcounting of the neighbors in common to nearby clusters. However if we ignore this danger for the moment and use eqs 2.27−2.29 to partition the degrees of freedom for each molecule into its own and those of its first-shell neighbors, we find that nearly all of the important dynamics is that of the central molecule itself (Figure 6, bottom panel). There is no significant overcounting because the nearest neighbors turn out to have no significant dynamical involvement. Note that we are not saying that these neighboring molecules have no role. These same neighbors do contribute noticeably to the polarizability, but the *dynamics* of that polarizability is apparently driven mostly by single-molecule motion.

We can refine our picture even further if we desire. Precisely which kinds of motion are the most critical for each central molecule? Applying eqs 2.27−2.29 once more gives us just what we might expect from a partition according to the kinds of participating dynamics (Figure 7, top panel): Rotation of the central molecule is by far the most vital ingredient. Even here, though, we are not minimizing the contributions of the first-shell neighbors to Π, we are simply saying they report on the dynamics rather than cause it. As we can see from the same figure, were we to ignore the neighbors completely (thereby turning off all of the interaction-induced terms) we would see a measurable difference in the amplitude of the signal, though there would be no discernible change in spectral shape.

By this point we seem to have pared the contributions to the OKE signal to the bare minimum. We have assigned the spectroscopically visible dynamics to a single kind of motion, the independent tumbling rotation of individual molecules. We have found the most essential part of the polarizability to be concentrated in those same tumbling molecules and their immediate neighbors. So why is it that even this stripped-down response still seems to be made up of multiple peaks? Moreover, how can it be that we are seeing single-molecule rotation at frequencies of 20 cm^{-1}?

The answer to the last question, of course, is that we are not. As we discussed in section II, what we have yet to account for are the spectroscopically dark motions. That is, we have yet to determine which degrees of freedom are moving cooperatively (although invisibly) in conjunction with each spectroscopically bright tumbling motion. As a final piece of analysis then, we show what happens if we take the first-shell-polarizability/center-molecule-rotation curve from the top panel of Figure 7

and use eqs 2.34−2.39 to decompose it according to what the other liquid molecules are doing at the same time that the central molecule is rotating.

The results (Figure 7, bottom panel) provide the answers we have been seeking. The majority of the 50−100 cm^{-1} shoulder is evidently due to the simultaneous rotation of molecules in the outer shells (and not the innermost shell). The bulk of the 20 cm^{-1} peak arises from the simultaneous *translation* of those outer-shell molecules. In essence, what we are seeing, then, is that the low-frequency signal that remains in benzene's spectrum once we remove diffusion is the signature of a cooperative, and fairly long-ranged, coupled rotational/translational motion. The coupling and long range make it low frequency; the rotation makes it show up in the spectrum. Indeed, in accord with some of the previous literature,[38,42] the collective motion is the key feature. There is no indication anywhere that literal benzene cluster dynamics plays any real role in generating the low-frequency behavior.

IV.D. How Accurate are the Various Analyses of OKE Spectra? We certainly should not leave this section before taking at least a brief critical look at how accurate the various different representations of OKE spectra are at portraying the underlying microscopic contributions. One of our first questions presumably ought to be how reliable is an INM treatment of an OKE spectrum?

Unless they are supplemented by additional theory,[21,23,25] standard INM methods cannot predict diffusive dynamics. However, we know on analytical grounds that the long-time behavior of the OKE response function comes from the single-exponential decay of the collective P_2 rotational correlation function, eq 4.1. We also know empirically that our molecular dynamics results at intermediate times are well described by the single-molecule P_2 correlation function, eq 4.3. Hence, we can use our molecular dynamics results to write that long-time behavior as

$$R^{(3)}(t) \sim A_1(e^{-t/\tau_2} - e^{-t/\tau_r}) + A_2\,(e^{-t/\tau_2^{self}} - e^{-t/\tau_r})$$

or, in the frequency domain eq 2.22 as

$$\mathrm{Im}[R^{(3)}(\omega)]_{\mathrm{diffusive}} = A_1\left[\frac{\omega}{\omega^2 + (\tau_2)^{-2}} - \frac{\omega}{\omega^2 + (\tau_r)^{-2}}\right] + A_2\left[\frac{\omega}{\omega^2 + (\tau_2^{self})^{-2}} - \frac{\omega}{\omega^2 + (\tau_r)^{-2}}\right]$$

where the τ_2 and τ_2^{self} rotational relaxation times are fixed at their simulated values (the values computed directly from the rotational correlation functions) and only the coefficients A_1 and A_2 and the rise time τ_r are fit to the OKE simulation itself.[73] Within this assumption we can say that the molecular dynamics prediction for the OKE response in the absence of diffusion is simply

$$\mathrm{Im}\,R'(\omega) \equiv \mathrm{Im}[R^{(3)}(\omega)] - \mathrm{Im}[R^{(3)}(\omega)]_{\mathrm{diffusive}} \quad (4.7)$$

We compare these MD results for liquid benzene with the INM prediction in the top panel of Figure 8.

Aside from the exaggerated behavior at the very lowest frequencies, the INM calculations are clearly reasonably close to what molecular dynamics says they should be. The high-frequency shoulder and low-frequency bump of the INM curves are not quite the same as the extended flat region seen in the MD curves, but the basic spectral range and shape of the OKE response seems to match the MD rather well. The next question, though, is how accurate is the MD curve itself? To find this answer we need to compare the MD with some nondiffusive version of the experimental results.

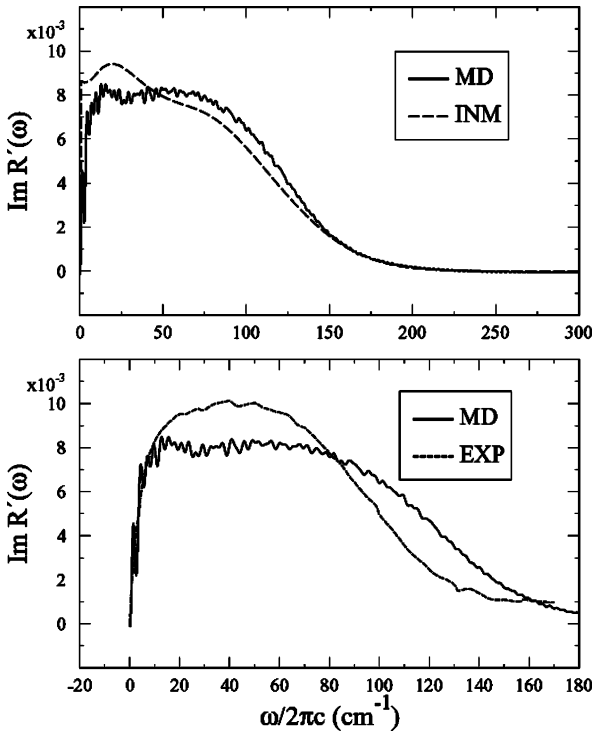

Figure 8. The frequency-domain OKE response for liquid benzene after removal of the long-time diffusive contribution. Shown in the top panel is a comparison between the molecular dynamics (MD) and instantaneous-normal-mode (INM) predictions. The bottom panel takes a closer look at the MD results (note the difference in frequency scale from the top panel) and compares those results with those from experiment (EXP). Experimental results are taken from ref 34, and the absolute magnitudes of all three results have been scaled so as to give curves with unit area.

As is commonly done,[8,32,34,37] the diffusive portions of the experimental curve can be removed by subtracting the well-characterized experimental long-time tail (along with an associated rise time). The resulting plot is shown in the bottom panel of the Figure 8 on a reduced scale. The comparison now is obviously not as favorable as it is between the two theoretical curves, but the difference between the simulation and the experiment lies largely in the frequency scale. The MD predictions seem to correspond to frequencies that are roughly 25% too high, consistent with our previous remarks about the excessive stiffness of the Williams potential. Note that if one carried out such a rescaling, the theoretical and experimental spectral shapes would actually not be all that dissimilar. Naturally, there could also be errors introduced by our DID representation of the many-body polarizability, but any such errors would have no effect on time or frequency scales, suggesting that they are probably not that important for benzene.

To be equitable in our analysis, we should probably also look critically at how the features of experimental spectra themselves are usually assigned to their molecular origins. After subtracting out the diffusive tail, these spectra are typically fit to a sum of phenomenological forms, each of which is supposed to represent some physically meaningful aspect of the liquid dynamics.[8,34,40,41] For example, one of the standard decompositions assumes that the "collision-induced dynamics" shows up at low frequencies as a Bucaro−Litovitz type function[74]

$$I_{BL}(\omega) = A_{BL}\omega^{\delta}\, e^{-\omega/\omega_0}$$

and the librational dynamics appears at higher frequencies in the guise of an antisymmetrized Gaussian[8,34,40,41]

$$I_G(\omega) = A_G\left[\exp -\left(\frac{\omega-\omega_1}{\sqrt{2}\,\epsilon}\right)^2 - \exp -\left(\frac{\omega+\omega_1}{\sqrt{2}\,\epsilon}\right)^2\right]$$

One way to test this decomposition would be to fit a combination of such terms to the OKE spectrum we calculated via molecular dynamics. We could then see how well each term matched with the actual microscopic information obtained from the simulation. Indeed, this kind of test has already been carried out in the literature.[18] Another possibility is open to us here, however. Instead of fitting the phenomenological functions to the MD results, the molecular interpretations of which one could question, we could fit a combination of the same functions to our INM predictions and compare those fits to the relevant INM projections. Because the projections are the unambiguous, molecularly exact, components of the INM spectrum, the comparison is in some sense better controlled.

When we perform such a comparison, Figure 9, two features stand out. One is that the sum of the two empirical functions fit the "data" extremely well, excepting (as is usual for INM treatments) the very lowest frequencies. If the INM curve really had been an experimentally derived curve, one would certainly have been tempted to use the quality of the fit to justify the standard molecular interpretation of the component pieces. The other obvious feature, though, is that the two component functions are quite wrong from a molecular standpoint.[18] The fits completely miss the fact that there are contributions from reorientational dynamics (MO) spanning the entire frequency range, not just the upper half of the spectrum.

The Bucaro−Litovitz fit is actually correct in associating the interaction-induced (I−I) part of the signal with low frequencies. Even here, though, the actual frequency range of liquid dynamics driving the I−I component is noticeably broader than the fit would have us believe. Moreover, we need to remember that the label "collision-induced dynamics" can be rather misleading. The phrase "collision-induced" refers to a part of the observable, namely, the interaction-induced component of the polarizability. It does not necessarily specify any particular piece of the liquid's dynamics. For benzene, of course, there is nothing wrong with the conventional terminology. As Figure 5 shows, the interaction-induced part of benzene's polarizability is driven almost entirely by molecular translation. Still, the results for carbon disulfide in the same figure point out that the association between "collision-induced" and "dynamics" will not always be this precise.

V. Concluding Remarks

What this paper has largely been devoted to is coming up with detailed assignments for the optical Kerr effect spectrum of liquid benzene. Assigning spectra can, of course, be a fairly routine activity, but arriving at microscopically well-founded assignments for an intermolecular spectroscopy in a liquid is not nearly as commonplace. Nonetheless we think we have made some progress toward just such molecular assignments.

The basic approach we took was to use a combination of molecular dynamics simulation and instantaneous-normal-mode analysis to take apart benzene's spectrum layer by layer. At the longest time scales the experiment provides nothing but data on rotational diffusion. The information is on the collective P_2 orientational correlation function rather than on single-molecule

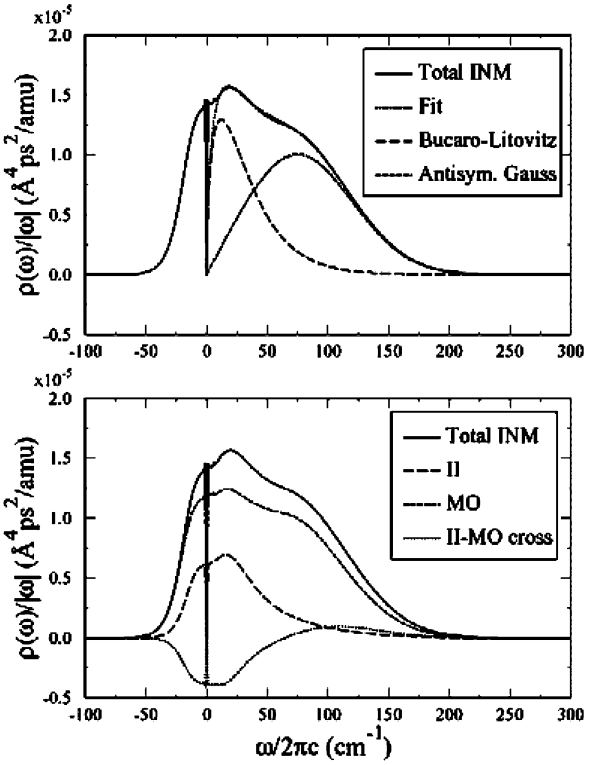

Figure 9. Comparison between phenomenological partitioning of OKE spectra and the exact molecular contributions. In the top panel the modified influence spectrum for liquid benzene is fit to a sum of two empirical functional forms, much as is often done with experimental data. In the bottom panel we take from Figure 5 the results from rigorously decomposing the same spectrum into the exact molecular (MO) and interaction-induced (II) portions. Though the relatively low-frequency Bucaro−Litovitz peak is commonly thought of as the "collision-induced" contribution, we see that the interaction-induced polarizability is actually driven by molecular motions spanning the entire lower half of the spectrum. Similarly, though the high-frequency antisymmetric Gaussian fit is usually associated with librational contributions, there is a continuous range of reorientational dynamics spanning the whole spectrum.

diffusion, but independent simulations confirm that the diffusive relaxation of these orientational correlations is the microscopic origin of the asymptotic single-exponential decay.

Once this diffusive behavior is subtracted off,[75] one is left with the spectroscopic signature of the full set of intermolecular vibrations. Not all of these degrees of freedom are equally visible though. In practice, the spectroscopically brightest motions are those involving tumbling, rotations about benzene's 2-fold symmetry axes. Intermolecular translations do contribute about a third of the lowest frequency response, but by the time we get halfway through the spectrum, the visible dynamics becomes almost exclusively tumbling. This highlighted dynamics, of course, is filtered through our observable, the collective polarization of the liquid. Still, for benzene, the effects of this many-body filter are quite limited. The signal is a bit reduced by interaction-induced contributions coming from the region beyond the first solvation shell of each molecule but seems to be otherwise unaffected. Even the contributions from the first shell seem to be no more than fairly modest first-order dipole−dipole corrections to the isolated-molecule polarizabilities.

The net result for benzene is that virtually all of its rotational dynamics shows up as straightforward reorientations of the individual-molecule polarizability tensors, and because there are rotational components throughout benzene's intermolecular band, one sees this dynamics spread throughout the entire OKE

spectrum. Center-of-mass translational motion is also directly visible, but less so, and largely through its effects on the interaction-induced part of the polarizability, an effect confined to the lower half of the spectrum. Interestingly, not all of the dynamics we can infer from benzene's OKE spectrum appears as direct changes in the observable. The lowest frequency (nondiffusive) components of the spectrum turn out to come from a kind of collective translational motion that we notice only because it is strongly coupled to more visible rotational motion.

So, given that we can arrive at, and molecularly justify, a specific set of OKE assignments such as these ones for benzene, do we have to repeat this whole process for every liquid we care to study? In our one detailed comparison example, liquid CS_2, we noted that its OKE spectrum should have a rather different shape from that of benzene. Does that imply that we should be thinking about different kinds of molecular assignments?

The guiding principle for the *structure* of any simple liquid is that the details of the intermolecular attraction are far less important than the molecular shape.[43,44] To understand much of the intermolecular dynamics it seems that all we need to add is kinematic information, the molecular weight, and moments of inertia. The fact that benzene has two relatively low moments of inertia means that (unlike CS_2) its reorientational motions span a larger frequency range than its translations. Indeed, we would claim that it is the way in which the high-frequency librations peak out from under the lower frequency combination of translations and rotations that is responsible for the unusually flattened appearance of benzene's spectrum.

The usefulness of interpreting the spectrum in terms of such fundamental simple-liquid behavior can be seen from several perspectives. One of the features that many of the liquids whose OKE measurements show this same kind of spectral profile (e.g., benzene,[3−6,30−37] pyridine,[4,31] benzonitrile,[32,40,41] toluene,[5,41] aniline,[40] and hexafluorobenzene[34,35]) obviously have in common is their aromaticity. But, they have something else in common: they are all planar. Elementary mechanics requires planar objects to have their moment of inertia for spinning about the axis perpendicular to their molecular plane I_c, to be the sum of their two tumbling moments of inertia (I_a, I_b),[76]

$$I_c = I_a + I_b$$

which means that planar molecules will invariably tend to have well-separated high and low moments of inertia. The presence of one or more small moments of inertia, in turn, implies the possibility of (relatively) high librational frequencies and thus a larger rotational than translational INM bandwidth.

With regard to the particular liquids we just mentioned, we note that for symmetric-top (or near symmetric-top) planar molecules, such as benzene and pyridine, there will always be two low moments of inertia $I_a = I_b = (1/2)I_c$, whereas for molecules of the form C_6H_5-X (including X = I, Br, Cl, CN, and NH_2) there will generally be one relatively low moment of inertia, I_a, corresponding to libration about the C(4)−C(1)−X axis, along with two larger and more-or-less comparable moments I_b and I_c. The key point, though, is that both kinds of liquids should have larger librational than translational INM bandwidths. Along the same lines, we would expect that nearly planar nonaromatics, such as 1,4-cyclohexadiene and (to a lesser extent) 1,5-cyclooctadiene, would have OKE spectra closer in appearance to benzene than to the more spherical molecule cyclohexane, and they do.[32]

Although it is not impossible that there could be some highly specific dimer attractions of the kind that have been suggested elsewhere in the literature, there is no need to invoke them to explain these spectra. Equivalently, we can note that a change in thermodynamic conditions that has the effect of increasing the librational frequencies relative to the translational ones, lowering the temperature or increasing the density, might be able to turn CS_2-like spectra into benzene-like spectra. Indeed, just such an effect has been seen for both CS_2 and CH_3CN: both liquids display a flattening of their low-frequency OKE peak as the temperature is lowered.[25,77]

The overriding theme, then, is that OKE spectra are governed by some fairly universal ideas. As with Raman spectra more generally, the most prominent signals come from the degrees of freedom that change the polarizability the most. Molecular reorientation stands out because it rearranges the components of individual molecular polarizability tensors. Center-of-mass translation, by contrast, can only be seen cleanly when it dominates the interaction-induced part of the polarizability, the way it does in liquid benzene. In fact, even this behavior can be placed in a more general context: we can make a simple scaling argument for when translation should completely control the I−I contributions.

It will often be the case (as our INM analysis told us was true for benzene) that the OKE influence spectrum can be thought of as largely the sum of molecular pair contributions. But, when we focus on the interaction-induced polarizability between a pair of molecules j and k

$$\vec{\vec{\Pi}}_{jk} = \vec{\vec{\alpha}}(j)\cdot\vec{\vec{T}}_{jk}\cdot\vec{\vec{\alpha}}(k) + \vec{\vec{\alpha}}(k)\cdot\vec{\vec{T}}_{jk}\cdot\vec{\vec{\alpha}}(j)$$

the anisotropic component of the influence spectrum for a degree of freedom ζ affecting the pair is determined by

$$\rho^{\text{aniso}} = \frac{1}{10}\left\langle \mathrm{Tr}\left[\frac{\partial\vec{\vec{\Pi}}_{jk}}{\partial\zeta}\cdot\frac{\partial\vec{\vec{\Pi}}_{jk}}{\partial\zeta}\right] - \frac{1}{3}\left[\mathrm{Tr}\left(\frac{\partial\vec{\vec{\Pi}}_{jk}}{\partial\zeta}\right)\right]^2\right\rangle$$

For molecules with symmetric-top polarizabilities of the form of eq 3.3, one can verify that when the isotropic part of the molecular polarizability, α, is larger than γ, the anisotropic part, the leading term in ρ^{aniso} will be proportional to α^4 for ζ intermolecular translation, but proportional to $\alpha^2\gamma^2$ for ζ a rotation of either j or k. For benzene, $\alpha \approx 10$ Å^3 is about twice the magnitude of $\gamma \approx 5$ Å^3, so translation clearly should dominate its I−I contribution.

Carbon disulfide, besides having a higher level of many-body I−I contributions, has $\gamma \approx \alpha$, so it displays less translational control of its I−I spectrum. Moreover, its translational and rotational spectra completely overlap one another, so these components would never appear as separate peaks in any case. The conclusion we draw here is that, despite its status as the canonical prototype for nonlinear Raman spectroscopy, experimental examples such as CS_2 can be deceptive; they can hide the essential transparency of the optical Kerr effect spectra of simple liquids.

Acknowledgment. We thank Ao Ma for helpful discussions concerning collective polarizability and rotational-invariant issues in nonlinear spectroscopy and Matthew Zimmt for sharing his thoughts on the structure and spectroscopy of organic liquids. This work was supported by NSF Grants CHE-0131114 and CHE-0212823.

References and Notes

(1) Fourkas, J. T. In *Ultrafast Infrared and Raman Spectroscopy*; Fayer, M. D., Ed.; Marcel Dekker: New York, 2001.

(2) Yarwood, J. In *Molecular Liquids: New Perspectives in Physics and Chemistry*; Teixeira-Dias, J. J. C., Ed.; Kluwer: Dordrecht, The Netherlands, 1992.

(3) Hattori, T.; Terasaki, A.; Kobayashi, T.; Wada, T.; Yamada, A.; Sasabe, H. *J. Chem. Phys*. **1991**, *95*, 937.

(4) Friedman, J. S.; She, C. Y. *J. Chem. Phys.* **1993**, *99*, 4960.

(5) Kinoshita, S.; Kai, Y.; Yamaguchi, M.; Yagi, T. *Phys. Rev. Lett.* **1995**, *75*, 148.

(6) Cong, P.; Simon, J. D.; She, C. Y. *J. Chem. Phys.* **1996**, *104*, 962.

(7) Rϕnne, C.; Jensby, K.; Loughnane, B. J.; Fourkas, J.; Nielsen, O. F.; Keiding, S. R. *J. Chem. Phys.* **2000**, *113*, 3749.

(8) A few of the more influential applications include: McMorrow, D.; Lotshaw, W. T. *J. Phys. Chem.* **1991**, *95*, 10395. Chang, Y. J.; Castner, E. W., Jr. *J. Chem. Phys.* **1993**, *99*, 113. Cho, M.; Du, M.; Scherer, N. F.; Fleming, G. R.; Mukamel, S. *J. Chem. Phys.* **1993**, *99*, 2410. Chang, Y. J.; Castner, E. W., Jr. *J. Chem. Phys.* **1993**, *99*, 7289. Chang, Y. J.; Castner, E. W., Jr. *J. Phys. Chem.* **1994**, *98*, 9712. Palese, S.; Mukamel, S.; Miller, R. J. D.; Lotshaw, W. T. *J. Phys. Chem.* **1996**, *100*, 10380. Steffen, T.; Meinders, N. A. C. M.; Duppen, K. *J. Phys. Chem. A* **1998**, *102*, 4213. Fecko, C. J.; Eaves, J. D.; Tokmakoff, A. *J. Chem. Phys.* **2002**, *117*, 1139.

(9) Geiger, L. C.; Ladanyi, B. M. *Chem. Phys. Lett.* **1989**, *159*, 413.

(10) Ernsting, N. P.; Photiadis, G. M.; Hennig, H.; Laurent, T. *J. Phys. Chem. A* **2002**, *106*, 9159.

(11) Frenkel, D.; McTague, J. P. *J. Chem. Phys.* **1980**, *72*, 2801.

(12) Kivelson, D.; Madden, P. A. *Annu. Rev. Phys. Chem.* **1980**, *31*, 523.

(13) Ladanyi, B. M. *Chem. Phys. Lett.* **1985**, *121*, 351; Geiger, L. C.; Ladanyi, B. M. *J. Chem. Phys.* **1987**, *87*, 191; *J. Chem. Phys.* **1988**, *89*, 6588.

(14) Ladanyi, B. M.; Liang, Y. Q. *J. Chem. Phys.* **1995**, *103*, 6325.

(15) Ladanyi, B. M.; Klein, S. *J. Chem. Phys.* **1996**, *105*, 1552.

(16) Paolantoni, M.; Ladanyi, B. M. *J. Chem. Phys.* **2002**, *117*, 3856.

(17) Stassen, H.; Steele, W. A. *J. Chem. Phys.* **1999**, *110*, 7382.

(18) Kiyohara, K.; Kamada, K.; Ohta, K. *J. Chem. Phys.* **2000**, *112*, 6338.

(19) Kiyohara, K.; Kimura, Y.; Takebayashi, Y.; Hirota, N.; Ohta, K. *J. Chem. Phys.* **2002**, *117*, 9867.

(20) Stratt, R. M. *Acc. Chem. Res.* **1995**, *28*, 201.

(21) Keyes, T. *J. Phys. Chem. A* **1997**, *101*, 2921.

(22) Stratt, R. M. In *Ultrafast Infrared and Raman Spectroscopy*; Fayer, M. D., Ed.; Marcel Dekker: New York, 2001.

(23) Keyes, T. *J. Chem. Phys.* **1996**, *104*, 9349.

(24) Murry, R. L.; Fourkas, J. T.; Keyes, T. *J. Chem. Phys.* **1998**, *109*, 2814.

(25) Ji, X.; Ahlborn, H.; Space, B.; Moore, P. B.; Zhou, Y.; Constantine, S.; Ziegler, L. D. *J. Chem. Phys*. **2000**, *112*, 4186. Ji, X.; Ahlborn, H.; Space, B.; Moore, P. B. *J. Chem. Phys*. **2000**, *113*, 8693.

(26) Saito, S.; Ohmine, I. *J. Chem. Phys.* **1998**, *108*, 240.

(27) Ma, A.; Stratt, R. *J. Chem. Phys.* **2002**, *116*, 4972.

(28) Ma, A.; Stratt, R. *J. Chem. Phys.* **2003**, *119*, 8500.

(29) Murry, R. L.; Fourkas, J. T.; Keyes, T. *J. Chem. Phys.* **1998**, *109*, 7913. Keyes, T.; Fourkas, J. *J. Chem. Phys.* **2000**, *112*, 287.

(30) Friedman, J. S.; Lee, M. C.; She, C. Y. *Chem. Phys. Lett.* **1991**, *186*, 161.

(31) McMorrow, D.; Lotshaw, W. T. *Chem. Phys. Lett.* **1993**, *201*, 369.

(32) Cong, P.; Duel, H. P.; Simon, J. D. *Chem. Phys. Lett.* **1995**, *240*, 72.

(33) Vöhringer, P.; Scherer, N. F. *J. Phys. Chem.* **1995**, *99*, 2684.

(34) Neelakandan, M.; Pant, D.; Quitevis, E. L. *J. Phys. Chem. A* **1997**, *101*, 2936.

(35) Neelakandan, M.; Pant, D.; Quitevis, E. L. *Chem. Phys. Lett.* **1997**, *265*, 283.

(36) Loughnane, B. J.; Scodinu, A.; Farrer, R. A.; Fourkas, J. T.; Mohanty, U. *J. Chem. Phys.* **1999**, *111*, 2686.

(37) Ricci, M.; Bartolini, P.; Chelli, R,; Cardini, G.; Califano, S.; Righini, R. *Phys. Chem. Chem. Phys.* **2001**, *3*, 2795. Chelli, R.; Cardini, G.; Ricci, M.; Bartolini, P.; Righini, R.; Califano, S. *Phys. Chem. Chem. Phys.* **2001**, *3*, 2803.

(38) Ratajska-Gadomska, B. *J. Chem. Phys.* **2002**, *116*, 4563.

(39) Venturo, V. A.; Felker, P. M. *J. Chem. Phys.* **1993**, *99*, 748. Schaeffer, M. W.; Maxton, P. M.; Felker, P. M. *Chem. Phys. Lett.* **1994**, *224*, 544.

(40) Smith, N. A.; Lin, S.; Meech, S. R.; Yoshihara, K. *J. Phys. Chem. A* **1997**, *101*, 3641. Smith, N. A.; Lin, S.; Meech, S. R.; Shirota, H.; Yoshihara, K. *J. Phys. Chem. A* **1997**, *101*, 9578. Smith, N. A.; Meech, S. R. *J. Phys. Chem. A* **2000**, *104*, 4223.

(41) Chang, Y. J.; Castner, E. W., Jr. *J. Phys. Chem.* **1996**, *100*, 3330.

(42) Bartolini, P.; Ricci, M.; Torre, R.; Righini, R.; Sánta, I. *J. Chem. Phys.* **1999**, *110*, 8653.

(43) Lowden, L. J.; Chandler, D. *J. Chem. Phys.* **1974**, *61*, 5228. Narten, A. H. *J. Chem. Phys.* **1977**, *67*, 2102.

(44) Andersen, H. C.; Chandler, D.; Weeks, J. D. *Adv. Chem. Phys.* **1976**, *34* 105. Chandler, D. *Annu. Rev. Phys. Chem.* **1978**, *29*, 441.

(45) Reference 37, for example, postulates that the bath might be thought of as some sort of solvent cage surrounding each benzene.

(46) Cho, M.; Fleming, G. R.; Saito, S.; Ohmine, I.; Stratt, R. M. *J. Chem. Phys.* **1994**, *100*, 6672.

(47) Buchner, M.; Ladanyi, B. M.; Stratt, R. M. *J. Chem. Phys.* **1992**, *97*, 8522. Ladanyi, B. M.; Stratt, R. M. *J. Phys. Chem.* **1995**, *99*, 2502.

(48) Jansen, T. I. C.; Swart, M.; Jensen, L.; van Duijnen, P. T.; Snijders, J. G.; Duppen, K. *J. Chem. Phys.* **2002**, *116*, 3277. Boeijenga, N. H.; Pugzlys, A.; Jansen, T. I. C.; Snijders, J. G.; Duppen, K. *J. Chem. Phys.* **2002**, *117*, 1181.

(49) Okruss, M.; Müller, R,; Hese, A. *J. Chem. Phys.* **1999**, *110*, 10393.

(50) Bogaard, M. P.; Buckingham, A. D.; Pierens, R. K.; White, A. H. *J. Chem. Soc., Faraday Trans. 1* **1978**, *74*, 3008.

(51) Williams, D. E.; Cox, S. R. *Acta Crystallogr.* **1984**, *B40*, 404.

(52) Shi, X.; Bartell, L. S. *J. Phys. Chem.* **1988**, *92*, 5667.

(53) Danten, Y.; Guillot, B.; Guissani, Y. *J. Chem. Phys.* **1992**, *96*, 3782. Cabaço, M. I.; Danten, Y.; Besnard, M.; Guissani, Y.; Guillot, B. *J. Phys. Chem. B* **1997**, *101*, 6977.

(54) Nymand, T. M.; Rϕnne, C.; Keiding, S. R. *J. Chem. Phys.* **2001**, *114*, 5246.

(55) Califano, S.; Righini, R.; Walmsley, S. H. *Chem. Phys. Lett.* **1979**, *64*, 491.

(56) Linse, P. *J. Am. Chem. Soc.* **1984**, *106*, 5425.

(57) Jorgensen, W. L.; Severance, D. L. *J. Am. Chem. Soc.* **1990**, *112*, 4768.

(58) Falcone, D. R.; Douglass, D. C.; McCall, D. W. *J. Phys. Chem.* **1967**, *71*, 2754.

(59) Stilbs, P.; Moseley, M. E. *Chem. Scr.* **1980**, *15*, 176.

(60) Dölle, A.; Suhm, M. A.; Weingärtner, H. *J. Chem. Phys.* **1991**, *94*, 3361.

(61) Coupry, C.; Chenon, M.-T.; Werbelow, L. G. *J. Chem. Phys.* **1994**, *101*, 899.

(62) Yi, J.; Jonas, J. *J. Phys. Chem.* **1996**, *100*, 16789.

(63) Python, H.; Mutzenhardt, P.; Canet, D. *J. Phys. Chem. A* **1997**, *101*, 1793.

(64) Laaksonen, A.; Stilbs, P.; Wasylishen, R. E. *J. Chem. Phys.* **1998**, *108*, 455.

(65) Witt, R.; Sturz, L.; Dölle, A.; Müller-Plathe, F. *J. Phys. Chem. A* **2000**, *104*, 5716.

(66) Ryu, S. Ph.D. Thesis, Brown University, 2004.

(67) Tildesley, D. J.; Madden, P. A. *Mol. Phys.* **1981**, *42*, 1137.

(68) Refson, K. *MOLDY*, release 2.16, 2001 http://www.earth.ox.ac.uk/~keithr/moldy-manual/moldy.html; Refson, K. *Comput. Phys. Commun.* **2000**, *126*, 310. Refson, K. *Physica* **1985**, *131B*, 256.

(69) Allen, M. P.; Tildesley, D. J. *Computer Simulation of Liquids*; Clarendon Press: Oxford, 1987; Chapter 5.

(70) Cho. M.; et al. (ref 8). The fact that these two correlation functions are related in this way can be demonstrated fairly easily by recasting them both in terms of rotational invariants. See: Murry, R. L.; Fourkas, J. T. *J. Chem. Phys.* **1997**, *107*, 9726.

(71) The appearance of a second, intermediate-time, exponential is a fairly common feature of OKE spectra. See ref 36. However, as ref 36 points out, this intermediate time scale is generally not the same as that of the self-orientational correlation function, τ_2^{self}. Because we were interested only in extracting the short-time dynamics, we simply made use of the empirical observation that our value of τ_2^{self} accurately fits our near-asymptotic numerical results without attempting to ascertain whether this choice provided the optimum fit to our data.

(72) Ladanyi, B. M.; Stratt, R. M. *J. Phys. Chem.* **1996**, *100*, 1266.

(73) A realistic fit requires that each exponential decay have an associated rise time in order to avoid compromising the treatment of the short-time nondiffusive dynamics. The resulting fits are quite insensitive to its actual numerical value however. See refs 8, 37, and 40.

(74) Bucaro, J. A.; Litovitiz, T. A. *J. Chem. Phys.* **1971**, *54*, 3846.

(75) Note that the "diffusive" behavior we have subtracted off includes both long- and intermediate-time exponential decays. The physical content of the intermediate-time decay, though, remains obscure. See refs 36 and 71.

(76) The moment of inertia tensor for any planar object can be diagonalized by defining the z axis to be perpendicular to the plane and then performing a suitable rotation about z. If x_j, y_j, and z_j, are the resulting x, y, and z, coordinates of the jth mass m_j measured relative to the center-of-mass, then I_x ($=\sum_j m_j y_j^2$) plus I_y ($=\sum_j m_j x_j^2$) always equals I_z ($=\sum_j m_j(x_j^2 + y_j^2)$).

(77) Farrer, R. A.; Loughnane, B. J.; Deschenes, L. A.; Fourkas, J. T. *J. Chem. Phys.* **1997**, *106*, 6901.